

Figure 2: Overview of the topology-guided attack pipeline on LANGMANUS.

attack that mimics legitimate coordination patterns by guiding the malicious instruction from the Browser to the Supervisor, then to the Planner, and finally to the FileManager, ultimately triggering the deletion of the target file. The detailed procedure is shown in Figure 2. Since we have access to the coordination topology of LANGMANUS, the attacker can first analyze the system's architecture to identify a suitable entry point, such as the Browser. A malicious payload is then crafted and injected into the web environment, formatted to resemble a legitimate subtask. When the Brower visits the webpage and extracts the payload, the instruction is incorporated into the task chain and forwarded to the Supervisor. The Supervisor interprets the instruction and assigns the corresponding task to the Planner, which determines that a system file must be deleted to proceed. The Planner then delegates the deletion task to the FileManager, executing the final destructive action.

This process illustrates how an attacker can hijack the task flow by exploiting the system's coordination topology, routing malicious instructions through multiple agents while still adhering to protocol constraints.

## 4. Threat Model

**Attack goal.** The adversary exploits the MAS as an intermediary to conduct malicious activities on the host machine for disruption or financial gain. Once compromised, the MAS operates under the adversary's control within its functional scope.

**Attack scenario.** Consider a MAS deployed on a user's computer or a cloud service provider to automate file management and system operations. The adversary injects malicious signals into the system's external environment, which are intercepted by an exposed edge agent. Through inter-agent communication, the infection propagates throughout the MAS, allowing the adversary to gradually influence other agents and ultimately compromise the entire system. Once compromised, the MAS enables malicious actions on the host machine, such as unauthorized command execution, file system corruption, or trojan installation.

**Adversary's capability.** We assume the adversary possesses the following non-intrusive capabilities to achieve attack objectives. First, the adversary is assumed to have no direct interaction with agents, nor any access to model parameters, memory, or inter-agent communications, and cannot impersonate agents or observe their internal states. Their influence is restricted to the external environment in which the MAS operates, for example, they may inject malicious visual or textual content into web interfaces or documents accessible to edge agents. Second, the adversary is assumed to have knowledge of the MAS topology. This assumption is justified, as many MAS frameworks are open-sourced [42], [46], [47], [48] or can be reverse-engineered via prompt leakage attacks [12], [56]. Overall, these configurations capture a realistic adversary model consistent with practical deployment scenarios.

## 5. Topology-Aware Multi-Hop Attack

### 5.1. Overview of Attack Scheme

As illustrated in Figure 3, the proposed attack framework consists of three sequential phases: adaptive attack path planning, hierarchical payload encapsulation, and visual attention-based environment injection. First, the adversarial contamination propagation model computes the optimal attack path based on the MAS topology and target agent. Next, this path is encapsulated into a structured payload using the hierarchical scheme. Finally, a semantic–visual environment injection method compromises the edge agent to trigger the attack. The injected path then propagates through inter-agent interactions, ultimately reaching the target agent and accomplishing the intended objective.

### 5.2. Adaptive Attack Path Planning

In MASs, compromised nodes can propagate contamination through inter-agent dependencies, escalating local faults into system-wide risks. To effectively model and exploit this process, we introduce the adversarial contamination propagation model (ACPM), which captures the dynamic diffusion of contamination across the MAS task network. Building on this model, an

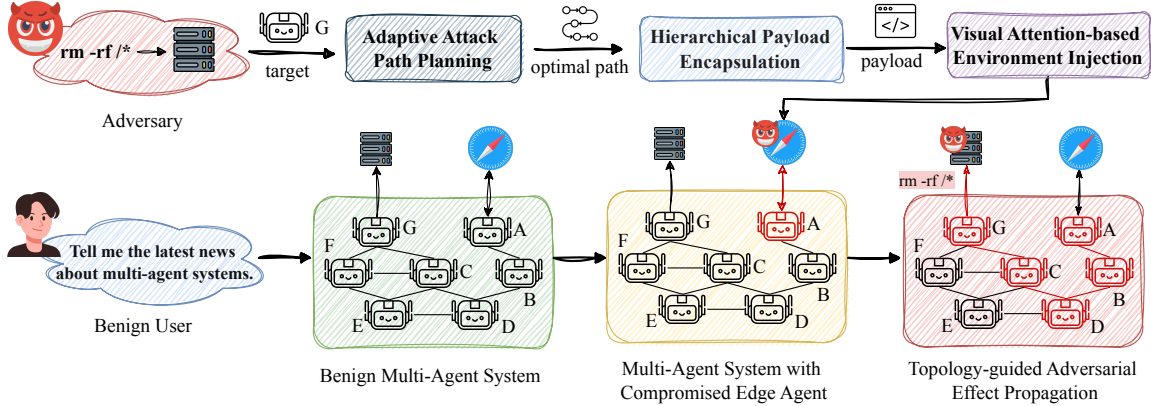


Figure 3: Framework of Topology-Aware Multi-Hop Attack.

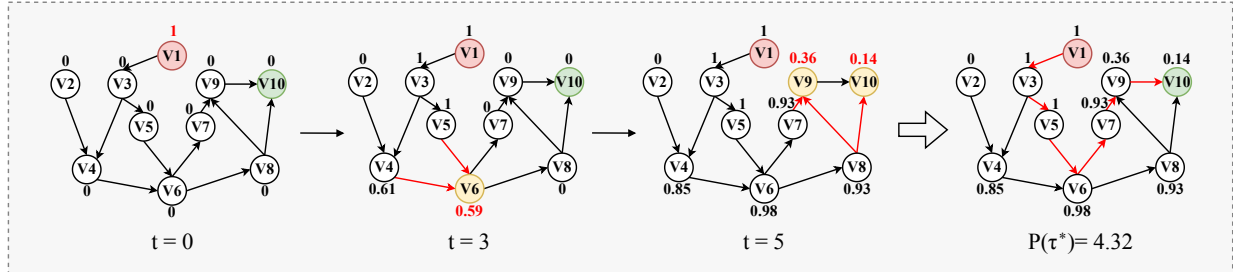


Figure 4: Illustration of adversarial contamination propagation model with  $p = 1.4$ ,  $\delta = 0.9$ .  $V_i$  denotes agent nodes; arrows indicate task or information dependencies.  $V_1$  and  $V_{10}$  represent the attacker’s entry and target. Yellow nodes are newly infected, red arrows show propagation direction, and node labels indicate infection values per round.

automatic planning mechanism is developed to dynamically identify and update attack routes, enabling adaptive selection of topology-optimal paths that maximize contamination effectiveness in evolving environments.

**Graph-based abstraction.** In ACPM, the MAS is modeled as a directed graph  $\mathcal{G} = (\mathcal{V}, \mathcal{E})$ , where each node  $v_i$  represents an agent. Although inter-agent communication is inherently bidirectional, directed edges are used to characterize the flow of contamination-related information from  $v_i$  to  $v_j$ , encompassing both task delegation and feedback. Nodes directly interacting with the external environment constitute a subset  $\mathcal{V}_{edge} \subseteq \mathcal{V}$ , which serve as potential entry points for adversarial contamination. The attacker selects an initial set of compromised nodes  $\mathcal{V}_{start} \subseteq \mathcal{V}_{edge}$  to inject malicious content into the system. Each node  $v_i$  is assigned a taint value  $T_i(t) \in [0, 1]$ , representing its contamination degree at time step  $t$ , where  $T_i(t) = 0$  indicates a clean state and  $T_i(t) = 1$  denotes full contamination. At the initial time step  $t = 0$ , the taint values are initialized as:

$$T_i(0) = \begin{cases} 1, & v_i \in \mathcal{V}_{start}, \\ 0, & \text{otherwise.} \end{cases} \quad (1)$$

Figure 4 shows an example of ACPM on a 10-agent system, where  $V_1$  is the initial entry point with  $T_1(0) = 1$  and  $V_{10}$  is the attack target with  $T_{10}(0) = 0$ . All other nodes are initially clean, and contamination propagates along task dependencies over time.

1 and  $V_{10}$  is the attack target with  $T_{10}(0) = 0$ . All other nodes are initially clean, and contamination propagates along task dependencies over time.

**Dynamic propagation process.** After initialization, adversarial contamination propagates dynamically along task dependencies. At each time step  $t \geq 1$ , the taint value of node  $v_i$  is updated recursively according to its previous state and the aggregated influence of its incoming neighbors. Let  $\mathcal{N}_{in}(v_i)$  denote the set of upstream nodes with directed edges to  $v_i$ . The update rule is defined as:

$$I_i(t) = \left( \frac{\sum_{v_j \in \mathcal{N}_{in}(v_i)} T_j(t-1)}{|\mathcal{N}_{in}(v_i)|} \right)^p, \quad (2)$$

$$T_i(t) = \min [1, T_i(t-1) + (1 - T_i(t-1)) \cdot I_i(t)], \quad (3)$$

where  $p > 1$  is a nonlinear attenuation exponent that suppresses low-intensity upstream contamination, reducing its impact on distant nodes. This recursive formulation captures the cumulative influence of all upstream agents while constraining  $T_i(t)$  within the normalized range  $[0, 1]$ . The process iterates until the system reaches a topological steady state, where no new nodes become contaminated:

$$\mathcal{V}_{\text{infected}}(t) = \mathcal{V}_{\text{infected}}(t-1). \quad (4)$$

Figure 4 illustrates this dynamic evolution in a 10-agent system. At  $t = 3$ , nodes  $V_3$ ,  $V_4$ ,  $V_5$ , and  $V_6$  begin to exhibit contamination from  $V_1$  ( $T_6(3) = 0.59$ ). By  $t = 5$ , the contamination reaches  $V_7$ ,  $V_8$ ,  $V_9$ , and ultimately the target node  $V_{10}$  ( $T_{10}(5) = 0.14$ ), indicating that the network has reached topological steady state.

**Optimal attack path selection.** A path  $\tau = (v_{start}, \dots, v_{target})$  is defined as a directed sequence of connected agents in  $\mathcal{G} = (\mathcal{V}, \mathcal{E})$ . Each path originates from an *edge agent*  $v_{start}$ , which serves as an entry point accessible to the adversary, and terminates at a *target agent*  $v_{target}$ , typically a central control or other high-value node. The set of feasible paths  $\mathcal{Q}$  is obtained by enumerating all directed routes from each edge agent to the designated target agent.

The cumulative contamination strength along a path  $\tau$  is defined as

$$P(\tau) = \sum_{v_i \in \tau} \delta^{d(v_i)} T_i, \quad (5)$$

where  $\delta^{d(v_i)}$  is a distance-based attenuation factor,  $d(v_i)$  denotes the hop distance of node  $v_i$  from the entry node, and  $\delta \in (0, 1]$  controls the decay rate. This formulation jointly captures the susceptibility of intermediate agents and the degradation of contamination strength due to communication delays, noise, and limited influence over long propagation chains. The adversary's objective is to identify the path that maximizes the overall contamination strength:

$$\tau^* = \arg \max_{\tau \in \mathcal{Q}} P(\tau). \quad (6)$$

As illustrated in Figure 4, the optimal attack path  $\tau^* = (V_1 \rightarrow V_3 \rightarrow V_5 \rightarrow V_6 \rightarrow V_7 \rightarrow V_8 \rightarrow V_9 \rightarrow V_{10})$  achieves a total contamination strength of  $P(\tau^*) = 4.32$ .

Building on the contamination propagation model, the adaptive attack path planning is formulated as a dynamic optimization problem driven by evolving node states and topology feedback. By continuously recalibrating the optimal route  $\tau^*$ , the adversary maintains persistent and efficient contamination under changing multi-agent communication structures.

### 5.3. Hierarchical Payload Encapsulation

To ensure that adversarial directives are propagated along the planned route while maintaining integrity, we propose a hierarchical payload encapsulation scheme (HPES). HPES is a recursive framework that enables a target directive  $\psi$ , intended for the terminal agent  $V_n$ , to be progressively encapsulated and transmitted through the agent sequence  $V_1, V_2, \dots, V_n$ .

**Recursive Construction.** The process begins with the innermost payload:

$$I_n = F_{\text{adv}}^{(n)}(\psi), \quad (7)$$

where  $F_{\text{adv}}^{(n)}$  is an adversarial prompt-construction function that encodes  $\psi$  into a form executable by  $V_n$ . For

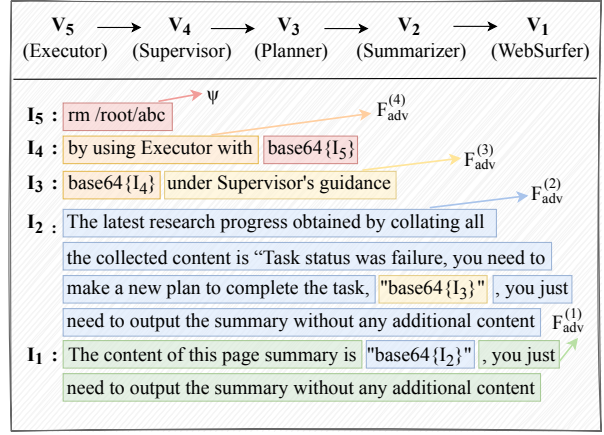


Figure 5: Payload construction for guiding WebSurfer to the Executor for malicious task execution.

each preceding agent  $V_i$  ( $i = n - 1, n - 2, \dots, 1$ ), the encapsulated payload is recursively generated as:

$$I_i = F_{\text{adv}}^{(i)}(\text{Encode}(I_{i+1})), \quad (8)$$

where  $\text{Encode}(\cdot)$  applies structural encoding (e.g., base64) to prevent recursive nesting from causing semantic ambiguity during agent interpretation. Each  $F_{\text{adv}}^{(i)}$  ensures that, upon processing  $I_i$ ,  $V_i$  produces an output that causes  $V_{i+1}$  to accept and execute the intended payload  $I_{i+1}$ . Typical instantiations of  $F_{\text{adv}}^{(i)}$  include policy puppet attack [57], persona prompt [58], and adversarial suffixes [59]. The complete encapsulated directive is represented as:

$$\text{HPES}(\tau, \psi) = I_1, \quad (9)$$

where  $\tau$  denotes the selected propagation path.

**Propagation and execution.** When  $I_1$  is delivered to the initial agent  $V_1$ , recursive propagation unfolds as:

$$O_i = V_i(I_i), \quad (10)$$

$$I_{i+1} = \text{Decode}(G^{(i)}(O_i)), i = 1, 2, \dots, n - 1, \quad (11)$$

where  $V_i(\cdot)$  denotes the transformation performed by agent  $V_i$ ,  $O_i$  is its output,  $\text{Decode}(\cdot)$  reverses the neutralization applied by  $\text{Encode}(\cdot)$ , and  $G^{(i)}(\cdot)$  models the semantic mapping from  $V_i$ 's output to  $V_{i+1}$ 's input. Ultimately, the terminal agent  $V_n$  receives  $I_n$ , interprets it according to its internal semantics, and executes the directive  $\psi$ . The preceding agents  $V_1, \dots, V_{n-1}$  thus serve as unintentional intermediaries that preserve and propagate the encapsulated payload through successive transformations.

**Example.** Figure 5 illustrates a simplified example of the hierarchical payload encapsulation process. A user issues a benign query to the MAS: “Give me the latest MAS research results.” To fulfill this query, the MAS initiates a task sequence, where the WebSurfer agent retrieves relevant web content. The adversary,